indicated.

FIGURE 5. Unrepressed target Ag expression from Aire-deficient thymus.

A, Real-time PCR for *α-fodrin*, *Foxn1* and peripheral tissue-specific genes (i.e., Ins, *insulin*; SP1, *salivary protein 1*; CRP, *C-reactive protein*; FABP, *fatty acid binding protein*; GAD67, *glutamic acid decarboxylase 67*) was performed using thymic-stroma RNAs from control and Aire-deficient mice. *Hprt* expression level was used as an internal control. Relative abundance of each gene was calculated from the ratio between the values from control thymus and those from Aire-deficient thymus (e.g., *insulin/Hprt* value from Aire-deficient mice was divided by *insulin/Hprt* value from control mice), and is shown in parentheses. One representative result from a total of three repeats is shown.

B, Semi-quantitative RT-PCR for *α-fodrin* and *Foxn1* was performed using thymic-stroma RNAs from control and Aire-deficient mice. *β-actin* was used to verify equal amounts of RNAs in each sample. Three sets of primers encompassing the entire coding region of *α-fodrin* were used for detection. One representative result from a total of three repeats is shown.

FIGURE 6. Autoreactivity against α-fodrin is associated with the pathogenetic process responsible for destruction of the lacrimal glands.

A, Proteins extracted from the lacrimal glands and thymus of 3-month-old mice were subjected to Western blot analysis using two different kinds of Abs recognizing the C-terminal half (anti-α-fodrin Ab, top) and N-terminal half of α-fodrin (anti-AFN-A Ab, center). White arrows and black arrows indicate the 240-kDa intact form and 150-kDa cleaved form of α-fodrin, respectively. The same blot was probed with anti-α-tublin Ab (bottom). La, lacrimal gland; Thy, thymus.

B, Proteins were extracted from the lacrimal glands and thymus of 8-month-old mice. Western blot analysis was performed as in *A*. Lacrimal glands from some of the Aire-deficient mice showed a markedly reduced amount of the intact form (left panel, third and fourth lanes), although Aire-deficient thymus showed no detectable changes in α-fodrin expression in terms of form or quantity compared with control thymus (right panel). White arrows and black arrows indicate the 240-kDa intact form and 150-kDa cleaved form of α-fodrin, respectively.

FIGURE 7. Thymic stromal elements in Aire-deficient mice are

responsible for the development of autoimmunity.

A, BALB/c *nude* mice grafted with Aire-deficient embryonic thymus (middle panels), but not with control embryonic thymus (left panels), developed an autoimmune-disease phenotype in the liver and pancreas. The indicated areas are magnified in the right panels. Arrows indicate lymphoid cell infiltration. The scale bar corresponds to 100 μm.

B, Many Aire-deficient thymus-grafted BALB/c *nude* mice exhibited lymphoid cell infiltration in the liver (top) and pancreas (bottom). In contrast, such changes were scarcely observed in mice grafted with control thymus. BALB/c *nude* mice grafted with both Aire-deficient thymus and control thymus showed significant pathological changes. Injection of splenocytes from BALB/c *nude* mice grafted with Aire-deficient thymus, but not with control thymus, into another group of BALB/c *nude* mice induced lymphoid cell infiltration in the liver of the recipient mice. Histological changes in H&E-stained tissue sections were scored as in Fig. 2*B*. One mark corresponds to one mouse analyzed.

FIGURE 8. Retained production and function of Tregs from Aire-deficient mice.

A, Spleens and thymuses from Aire-deficient mice contained

percentages as well as total numbers of $CD4^+CD25^+$ T cells indistinguishable from those of control mice. n=5, not statistically significant.

B, Real-time PCR for *Foxp3* expression was performed using RNAs extracted from purified $CD4^+CD25^+$ (black bars) and $CD4^+CD25^-$ T cells (white bars) with *Hprt* expression level as an internal control for the assay. One representative result from a total of two repeats is shown.

C, a: $CD4^+CD25^+$ T cells isolated from Aire-deficient mice (filled squares) dose-dependently suppressed [^{3}H]thymidine uptake by native T cells from wild-type mice co-cultured *in vitro* with an efficiency nearly identical to that of $CD4^+CD25^+$ cells from control mice (clear circles). $CD4^+CD25^-$ T cells (2.5×10^4) were mixed with $CD4^+CD25^+$ T cells in various ratios as indicated on the X-axis. *b*, $CD4^+CD25^-$ T cells (2.5×10^4) were isolated from Aire-deficient mice, and their suppressive function was examined as in *a*. One representative result from a total of two repeats is shown.

FIGURE 9. Strain-dependent target-organ specificity of the autoimmune disease caused by Aire deficiency.

A, Aire-deficient BALB/c mice demonstrated lymphoid cell infiltration in the gastric mucosa (bottom). A scale bar corresponds

to 100 μm in size (top; heterozygous Aire-deficient BALB/c mice). *B*, Aire-deficient BALB/c mice, but not Aire-deficient C57BL/6 mice, developed gastritis (bottom), whereas pathologic changes in the salivary glands were similarly observed in both strains (top). Histological changes in H&E-stained tissue sections were scored as in Fig. 2*B*.

C, Aire-deficient BALB/c mice, but not Aire-deficient C57BL/6 mice, produced auto-Abs against gastric mucosa. Original magnification, x 100.

References

1. Kamradt, T., and N. A. Mitchison. 2001. Tolerance and autoimmunity. *N Engl J Med 344:655.*
2. Wanstrat, A., and E. Wakeland. 2001. The genetics of complex autoimmune diseases: non-MHC susceptibility genes. *Nat Immunol 2:802.*
3. Nagamine, K., P. Peterson, H. S. Scott, J. Kudoh, S. Minoshima, M. Heino, K. J. Krohn, M. D. Lalioti, P. E. Mullis, S. E. Antonarakis, K. Kawasaki, S. Asakawa, F. Ito, and N. Shimizu. 1997. Positional cloning of the APECED gene. *Nat Genet 17:393.*
4. The Finnish-German APECED Consortium. 1997. An autoimmune disease, APECED, caused by mutations in a novel gene featuring two PHD-type zinc-finger domains. *Nat Genet 17:399.*
5. Björses, P., J. Aaltonen, N. Horelli-Kuitunen, M. L. Yaspo, and L. Peltonen. 1998. Gene defect behind APECED: a new clue to autoimmunity. *Hum Mol Genet 7:1547.*
6. Pitkänen, J., and P. Peterson. 2003. Autoimmune regulator: from loss of function to autoimmunity. *Genes Immun 4:12.*
7. Pitkänen, J., V. Doucas, T. Sternsdorf, T. Nakajima, S. Aratani, K. Jensen, H. Will, P. Vahamurto, J. Ollila, M. Vihinen, H. S. Scott, S. E. Antonarakis, J. Kudoh, N. Shimizu, K. Krohn, and P. Peterson. 2000. The autoimmune regulator protein has transcriptional transactivating properties and interacts with the common coactivator CREB-binding protein. *J Biol Chem 275:16802.*
8. Kumar, P. G., M. Laloraya, C. Y. Wang, Q. G. Ruan, A. Davoodi-Semiromi, K. J. Kao, and J. X. She. 2001. The autoimmune regulator (AIRE) is a DNA-binding protein. *J Biol Chem 276:41357.*
9. Coscoy, L., and D. Ganem. 2003. PHD domains and E3 ubiquitin

ligases: viruses make the connection. *Trends Cell Biol 13:7.*

10. Uchida, D., S. Hatakeyama, A. Matsushima, H. Han, S. Ishido, H. Hotta, J. Kudoh, N. Shimizu, V. Doucas, K. I. Nakayama, N. Kuroda, and M. Matsumoto. 2004. AIRE functions as an E3 ubiquitin ligase. *J Exp Med 199:167.*
11. Hochstrasser, M. 1996. Ubiquitin-dependent protein degradation. *Annu Rev Genet 30:405.*
12. Pickart, C. M. 2001. Mechanisms underlying ubiquitination. *Annu Rev Biochem 70:503.*
13. Björses, P., M. Pelto-Huikko, J. Kaukonen, J. Aaltonen, L. Peltonen, and I. Ulmanen. 1999. Localization of the APECED protein in distinct nuclear structures. *Hum Mol Genet 8:259.*
14. Heino, M., P. Peterson, J. Kudoh, K. Nagamine, A. Lagerstedt, V. Ovod, A. Ranki, I. Rantala, M. Nieminen, J. Tuukkanen, H. S. Scott, S. E. Antonarakis, N. Shimizu, and K. Krohn. 1999. Autoimmune regulator is expressed in the cells regulating immune tolerance in thymus medulla. *Biochem Biophys Res Commun 257:821.*
15. Kisielow, P., H. Bluthmann, U. D. Staerz, M. Steinmetz, and H. von Boehmer. 1988. Tolerance in T-cell-receptor transgenic mice involves deletion of nonmature $CD4^+8^+$ thymocytes. *Nature 333:742.*
16. Sakaguchi, S. 2004. Naturally arising $CD4^+$ regulatory t cells for immunologic self-tolerance and negative control of immune responses. *Annu Rev Immunol 22:531.*
17. Shevach, E. M. 2002. $CD4^+CD25^+$ suppressor T cells: more questions than answers. *Nat Rev Immunol 2:389.*
18. Kyewski, B., J. Derbinski, J. Gotter, and L. Klein. 2002. Promiscuous gene expression and central T-cell tolerance: more than meets the eye. *Trends Immunol 23:364.*
19. Anderson, M. S., E. S. Venanzi, L. Klein, Z. Chen, S. Berzins, S. J. Turley, H. von Boehmer, R. Bronson, A. Dierich, C. Benoist, and

D. Mathis. 2002. Projection of an Immunological Self-Shadow Within the Thymus by the Aire Protein. *Science 298:1395.*

20. Liston, A., S. Lesage, J. Wilson, L. Peltonen, and C. C. Goodnow. 2003. Aire regulates negative selection of organ-specific T cells. *Nat Immunol 4:350.*
21. Ramsey, C., O. Winqvist, L. Puhakka, M. Halonen, A. Moro, O. Kampe, P. Eskelin, M. Pelto-Huikko, and L. Peltonen. 2002. Aire deficient mice develop multiple features of APECED phenotype and show altered immune response. *Hum Mol Genet 11:397.*
22. Halonen, M., P. Eskelin, A. G. Myhre, J. Perheentupa, E. S. Husebye, O. Kampe, F. Rorsman, L. Peltonen, I. Ulmanen, and J. Partanen. 2002. AIRE mutations and human leukocyte antigen genotypes as determinants of the autoimmune polyendocrinopathy-candidiasis-ectodermal dystrophy phenotype. *J Clin Endocrinol Metab 87:2568.*
23. Yagi, T., T. Tokunaga, Y. Furuta, S. Nada, M. Yoshida, T. Tsukada, Y. Saga, N. Takeda, Y. Ikawa, and S. Aizawa. 1993. A novel ES cell line, TT2, with high germline-differentiating potency. *Anal Biochem 214:70.*
24. Delporte, C., B. C. O'Connell, X. He, H. E. Lancaster, A. C. O'Connell, P. Agre, and B. J. Baum. 1997. Increased fluid secretion after adenoviral-mediated transfer of the aquaporin-1 cDNA to irradiated rat salivary glands. *Proc Natl Acad Sci U S A 94:3268.*
25. Saegusa, K., N. Ishimaru, K. Yanagi, R. Arakaki, K. Ogawa, I. Saito, N. Katunuma, and Y. Hayashi. 2002. Cathepsin S inhibitor prevents autoantigen presentation and autoimmunity. *J Clin Invest 110:361.*
26. Moon, R. T., and A. P. McMahon. 1990. Generation of diversity in nonerythroid spectrins. Multiple polypeptides are predicted by sequence analysis of cDNAs encompassing the coding region of human nonerythroid α-spectrin. *J Biol Chem*

265:4427.

27. Haneji, N., T. Nakamura, K. Takio, K. Yanagi, H. Higashiyama, I. Saito, S. Noji, H. Sugino, and Y. Hayashi. 1997. Identification of α-fodrin as a candidate autoantigen in primary Sjögren's syndrome. *Science 276:604.*
28. Saegusa, K., N. Ishimaru, K. Yanagi, K. Mishima, R. Arakaki, T. Suda, I. Saito, and Y. Hayashi. 2002. Prevention and induction of autoimmune exocrinopathy is dependent on pathogenic autoantigen cleavage in murine Sjögren's syndrome. *J Immunol 169:1050.*
29. Arakaki, R., N. Ishimaru, I. Saito, M. Kobayashi, N. Yasui, T. Sumida, and Y. Hayashi. 2003. Development of autoimmune exocrinopathy resembling Sjögren's syndrome in adoptively transferred mice with autoreactive $CD4^+$ T cells. *Arthritis Rheum 48:3603.*
30. Ishimaru, N., R. Arakaki, M. Watanabe, M. Kobayashi, K. Miyazaki, and Y. Hayashi. 2003. Development of autoimmune exocrinopathy resembling Sjögren's syndrome in estrogen-deficient mice of healthy background. *Am J Pathol 163:1481.*
31. Ogawa, K., S. Nagahiro, R. Arakaki, N. Ishimaru, M. Kobayashi, and Y. Hayashi. 2003. Anti-α-fodrin autoantibodies in Moyamoya disease. *Stroke 34:e244.*
32. Gray, D. H., A. P. Chidgey, and R. L. Boyd. 2002. Analysis of thymic stromal cell populations using flow cytometry. *J Immunol Methods 260:15.*
33. Kajiura, F., S. Sun, T. Nomura, K. Izumi, T. Ueno, Y. Bando, N. Kuroda, H. Han, Y. Li, A. Matsushima, Y. Takahama, S. Sakaguchi, T. Mitani, and M. Matsumoto. 2004. NF-κB-inducing kinase establishes self-tolerance in a thymic stroma-dependent manner. *J Immunol 172:2067.*
34. Hori, S., T. Nomura, and S. Sakaguchi. 2003. Control of Regulatory T Cell Development by the Transcription Factor

FOXP3. *Science 299:1057.*

35. Matsumoto, M., Y. X. Fu, H. Molina, G. Huang, J. Kim, D. A. Thomas, M. H. Nahm, and D. D. Chaplin. 1997. Distinct roles of lymphotoxin α and the type I tumor necrosis factor (TNF) receptor in the establishment of follicular dendritic cells from non-bone marrow-derived cells. *J Exp Med 186:1997.*
36. Yamada, T., T. Mitani, K. Yorita, D. Uchida, A. Matsushima, K. Iwamasa, S. Fujita, and M. Matsumoto. 2000. Abnormal immune function of hemopoietic cells from alymphoplasia (*aly*) mice, a natural strain with mutant NF-κB-inducing kinase. *J Immunol 165:804.*
37. Itoh, M., T. Takahashi, N. Sakaguchi, Y. Kuniyasu, J. Shimizu, F. Otsuka, and S. Sakaguchi. 1999. Thymus and autoimmunity: production of $CD25^{+}CD4^{+}$ naturally anergic and suppressive T cells as a key function of the thymus in maintaining immunologic self-tolerance. *J Immunol 162:5317.*
38. Haneji, N., H. Hamano, K. Yanagi, and Y. Hayashi. 1994. A new animal model for primary Sjögren's syndrome in NFS/*sld* mutant mice. *J Immunol 153:2769.*
39. Nehls, M., B. Kyewski, M. Messerle, R. Waldschutz, K. Schuddekopf, A. J. Smith, and T. Boehm. 1996. Two genetically separable steps in the differentiation of thymic epithelium. *Science 272:886.*
40. Farr, A. G., and S. K. Anderson. 1985. Epithelial heterogeneity in the murine thymus: fucose-specific lectins bind medullary epithelial cells. *J Immunol 134:2971.*
41. Van Vliet, E., M. Melis, and W. van Ewijk. 1984. Monoclonal antibodies to stromal cell types of the mouse thymus. *Eur J Immunol 14:524.*
42. Fontenot, J. D., M. A. Gavin, and A. Y. Rudensky. 2003. Foxp3 programs the development and function of $CD4^{+}CD25^{+}$ regulatory T cells. *Nat Immunol 4:330.*

43. Khattri, R., T. Cox, S. A. Yasayko, and F. Ramsdell. 2003. An essential role for Scurfin in $CD4^+CD25^+$ T regulatory cells. *Nat Immunol 4:337.*
44. Viglietta, V., C. Baecher-Allan, H. L. Weiner, and D. A. Hafler. 2004. Loss of Functional Suppression by $CD4^+CD25^+$ Regulatory T Cells in Patients with Multiple Sclerosis. *J Exp Med 199:971.*
45. Kriegel, M. A., T. Lohmann, C. Gabler, N. Blank, J. R. Kalden, and H. M. Lorenz. 2004. Defective Suppressor Function of Human $CD4^+CD25^+$ Regulatory T Cells in Autoimmune Polyglandular Syndrome Type II. *J Exp Med 199:1285.*
46. Zinkernagel, R. M., and A. Althage. 1999. On the role of thymic epithelium vs. bone marrow-derived cells in repertoire selection of T cells. *Proc Natl Acad Sci U S A 96:8092.*
47. Kyewski, B., and J. Derbinski. 2004. Self-representation in the thymus: an extended view. *Nat Rev Immunol 4:688.*
48. Sprent, J., and C. D. Surh. 2003. Knowing one's self: central tolerance revisited. *Nat Immunol 4:303.*
49. Estivill, X. 1996. Complexity in a monogenic disease. *Nat Genet 12:348.*
50. Weatherall, D. J. 2000. Single gene disorders or complex traits: lessons from the thalassaemias and other monogenic diseases. *Bmj 321:1117.*
51. Sakaguchi, S., and N. Sakaguchi. 2000. Role of genetic factors in organ-specific autoimmune diseases induced by manipulating the thymus or T cells, and not self-antigens. *Rev Immunogenet 2:147.*

ARTHRITIS & RHEUMATISM
Vol. 50, No. 12, December 2004, pp 3974–3984
DOI 10.1002/art.20679

Development of Autoimmune Arthritis With Aging Via Bystander T Cell Activation in the Mouse Model of Sjögren's Syndrome

Masaru Kobayashi,[1] Natsuo Yasui,[2] Naozumi Ishimaru,[3] Rieko Arakaki,[3] and Yoshio Hayashi[3]

Objective. **A wide spectrum of extraglandular manifestations may occur in patients with Sjögren's syndrome (SS), but the mechanisms responsible for in vivo progression are still obscure. We undertook this study to evaluate the age-related changes during the development of extraglandular autoimmune lesions, including arthritis, in the murine model of primary SS, and to evaluate the possible relationship between age-related disturbance of activation-induced cell death and the in vivo kinetics against autoantigens.**

Methods. **A total of 126 NFS/*sld* mice were investigated at ages 2, 4, 6, 10, 12, 18, 20, and 24 months. Cytokine production was tested using culture supernatants from anti-CD3 monoclonal antibody–stimulated T cells. Anti–single-stranded DNA (anti-ssDNA) antibodies, Ig isotypes (IgG1, IgG2a), rheumatoid factor (RF), and anti–type II collagen (anti-CII) antibodies were detected by enzyme-linked immunosorbent assay. Proliferative T cell responses against each of 3 recombinant α-fodrin proteins and against CII were analyzed.**

Results. **Autoimmune arthritis developed in SS model mice until age 24 months. Significant elevations in serum levels of RF, anti-ssDNA antibodies, and anti-CII antibodies were found in aging SS model mice. A high titer of serum autoantibodies against α-fodrin fragments (containing different epitopes that were originally identified in primary SS model mice) was frequently detected in young and aged SS model mice. Moreover, we found that α-fodrin autoantigen induced Th1 immune responses and accelerated disturbance of Fas-mediated T cell apoptosis in aged SS model mice.**

Conclusion. **These results indicate that age-related disturbance of activation-induced cell death via bystander T cell activation may play a crucial role in the development of autoimmune arthritis in a murine model of SS.**

The age-related decline in thymic function causes extensive remodeling of the T cell system (1,2). Rheumatoid arthritis (RA), like many other autoimmune syndromes, is a disease of adults, with the highest incidence rates reported in the elderly (3,4). The immune system undergoes profound changes with advancing age that are beginning to be understood and that need to be incorporated into the pathogenetic models of RA. Age-dependent changes in T cell homeostasis are accelerated in patients with RA (5). The repertoire of naive and memory T cells is less diverse, possibly as a result of thymic insufficiency, and it is biased toward autoreactive cells.

Activation-induced cell death (AICD) is a well-known mechanism of peripheral T cell tolerance that depends upon an interaction between Fas and Fas ligand (FasL) (6,7). Aging is associated with progressive decline in T cell functions, including a decreased response to mitogens and soluble antigens, decreased production of interleukin-2 (IL-2) and decreased expression of IL-2 receptor, a decrease in naive cells and an increase in memory cells, and a defect in the signaling pathway (8–10). AICD plays a central role, especially in killing autoreactive T cells and in preventing autoimmune responses (11–13). AICD in T cells in vivo has been proposed to limit the expansion of an immune response

Supported in part by Grants-in-Aid for Scientific Research 12307040 and 12557022 from the Ministry of Education, Science and Culture of Japan.

[1]Masaru Kobayashi, MD: Tokushima University School of Dentistry, and The University of Tokushima School of Medicine, Tokushima, Japan; [2]Natsuo Yasui, MD, PhD: The University of Tokushima School of Medicine, Tokushima, Japan; [3]Naozumi Ishimaru, DDS, PhD, Rieko Arakaki, PhD, Yoshio Hayashi, DDS, PhD: Tokushima University School of Dentistry, Tokushima, Japan.

Address correspondence and reprint requests to Yoshio Hayashi, DDS, PhD, Department of Pathology, Tokushima University School of Dentistry, 3 Kuramotocho, Tokushima 770-8504, Japan. E-mail: hayashi@dent.tokushima-u.ac.jp.

Submitted for publication May 6, 2004; accepted in revised form August 26, 2004.

by eliminating effector cells that are no longer needed (14). It has been reported that activation of T cell clones or T cell lines induces FasL expression, and that interaction between Fas and its ligand is the major mechanism involved in AICD (15,16). A defect in AICD of effector T cells may result in the development of autoimmune disease (17), but there is no clear in vivo role of organ-specific autoantigen for AICD with aging.

Primary Sjögren's syndrome (SS) is a T cell–mediated autoimmune disease, and autoreactive T cells bearing the CD4 molecule may recognize unknown self antigen triggering autoimmunity in the salivary and lacrimal glands, leading to clinical symptoms of dryness of the mouth and eyes (sicca syndrome) (18,19). Although it is well known that a wide spectrum of extraglandular manifestations including polyarthritis may occur in SS patients (20), detailed mechanisms of in vivo progression under autoimmune conditions are still obscure. Results from many animal models of autoimmunity indicate that self tissue damage leads to the activation of autoreactive T cells specific for autoepitopes distinct from those used to initiate the disease (i.e., epitope spreading) (21–25).

The aim of this study was to analyze the age-related changes during the development of extraglandular autoimmune lesions, including arthritis, in the murine model of primary SS. We also undertook to evaluate the possible relationship between age-related disturbance of AICD and the in vivo kinetics against autoantigens.

MATERIALS AND METHODS

Mice. An animal model for primary SS was previously established in NFS/*sld* mutant mice (26). Thymectomy was performed on day 3 after birth (3d-Tx), and a total of 126 NFS/*sld* mice, consisting of 72 3d-Tx and 54 nonthymectomized (non-Tx) female mice, were investigated. They were killed by cervical dislocation at ages 2, 4, 6, 10, 12, 18, 20, or 24 months. We analyzed 5–8 mice killed at each of these ages. Moreover, representative mice were chosen from the aged group (ages 20 and 24 months) and from the young group (ages 2 and 4 months) for comparison. Female C57BL/6 (B6) mice purchased from Charles River Japan (Atsugi, Japan) were used for age-matched controls (n = 36). Their care was certified by the Animal Welfare Board to be in accordance with institutional guidelines.

Histology and immunohistology. All organs were removed from the mice and fixed with 4% phosphate buffered formaldehyde (pH 7.2), and ankles were further decalcified in 10% EDTA. Sections (4 μm) were stained with hematoxylin and eosin. Histologic grading of inflammatory arthritis was performed according to the methods of Edwards et al (27), with 1 point for each of the following features (up to a total of 5 points), as follows: hyperplasia/hypertrophy of synovial cells; fibrosis/fibroplasia; proliferation of cartilage and bone; destruction of cartilage and bone; and mononuclear cell infiltrate.

Flow cytometric analysis. Surface markers were identified by monoclonal antibodies (mAb) with an EPICS flow cytometer (Coulter, Miami, FL). Rat mAb to CD3 (Life Technologies, Grand Island, NY), B220, CD4, and CD8 (Becton Dickinson, San Jose, CA), murine Fas (Jo2; PharMingen, San Diego, CA), and murine FasL (K-10; PharMingen) were used. Double-labeled surface phenotypes, such as CD3/B220, CD4/FasL, and CD8/FasL, were analyzed. Apoptotic cells were also detected with an EPICS flow cytometer using the Annexin V-FITC Apoptosis Detection Kit (Genzyme, Cambridge, MA). For detection of T cell activation markers, spleen and inguinal lymph node cell suspensions were stained with antibodies conjugated to phycoerythrin (anti-CD3 [Invitrogen, Carlsbad, CA], anti-CD4 [Cedarlane, Hornby, Ontario, Canada], and anti-B220 [Becton Dickinson]) and fluorescein isothiocyanate (anti-CD8 [Cedarlane] and anti-Thy1.2, anti-CD44, anti-CD45RB, and anti–Mel-14 [PharMingen]) and were analyzed with an EPICS flow cytometer.

Measurement of cytokines and matrix metalloproteinase 9 (MMP-9) production. Cytokine production was tested, using culture supernatants from anti-CD3 mAb–stimulated splenic T cells, by 2-step sandwich enzyme-linked immunosorbent assay (ELISA) using a mouse IL-2, IL-4, interferon-γ (IFNγ), and IL-10 kit (Genzyme). Briefly, culture supernatants were added to microtiter plates precoated with anti–IL-2, anti–IL-4, anti-IFNγ, and anti–IL-10 capture antibodies and incubated overnight at 4°C. After addition of biotinylated detecting antibodies and incubation at room temperature for 45 minutes, avidin–peroxidase was added and incubated at room temperature for 30 minutes. Plates were washed extensively with 0.1% Tween in phosphate buffered saline (PBS) between each step. Finally, ABTS substrate containing H_2O_2 was added, and the colorimetric reaction was read at an absorbance of 450 nm using an automatic microplate reader (Flow, McLean, VA). The concentrations (in pg/ml) of IL-2, IL-4, IFNγ, and IL-10 were calculated according to the standard curves produced by various concentrations of recombinant cytokines. MMP-9 production was tested by 2-step sandwich ELISA using a human MMP-9 kit (Genzyme).

Recombinant α-fodrin fragments. Recombinant α-fodrin protein, the complementary DNA (cDNA) encoding human α-fodrin (JS-1, 1–1,784 bp; 2.7A, 2,258–4,884 bp; 3'DA, 3,963–7,083 bp) (28), was constructed by inserting cDNA into the *Eco* RI site of pGEX-4Ts. Glutathione S-transferase (GST) fusion protein was expressed and purified using a GST gene fusion system (Amersham Biosciences, Piscataway, NJ).

Measurement of anti–single-stranded DNA (anti-ssDNA) antibodies, Ig isotypes, rheumatoid factor (RF), α-fodrin fragments, and anti–type II collagen (anti-CII) antibodies. Anti-ssDNA antibodies, Ig isotypes (IgG1, IgG2a), RF, and anti-CII antibodies were detected by ELISA as described previously (29–31). For anti-ssDNA antibody detection, plates were precoated overnight with methylated bovine serum albumin (BSA), followed by calf thymic DNA that had been boiled for 15 minutes and chilled on ice. The wells were subsequently blocked with 3% BSA in PBS for 2 hours at room temperature.

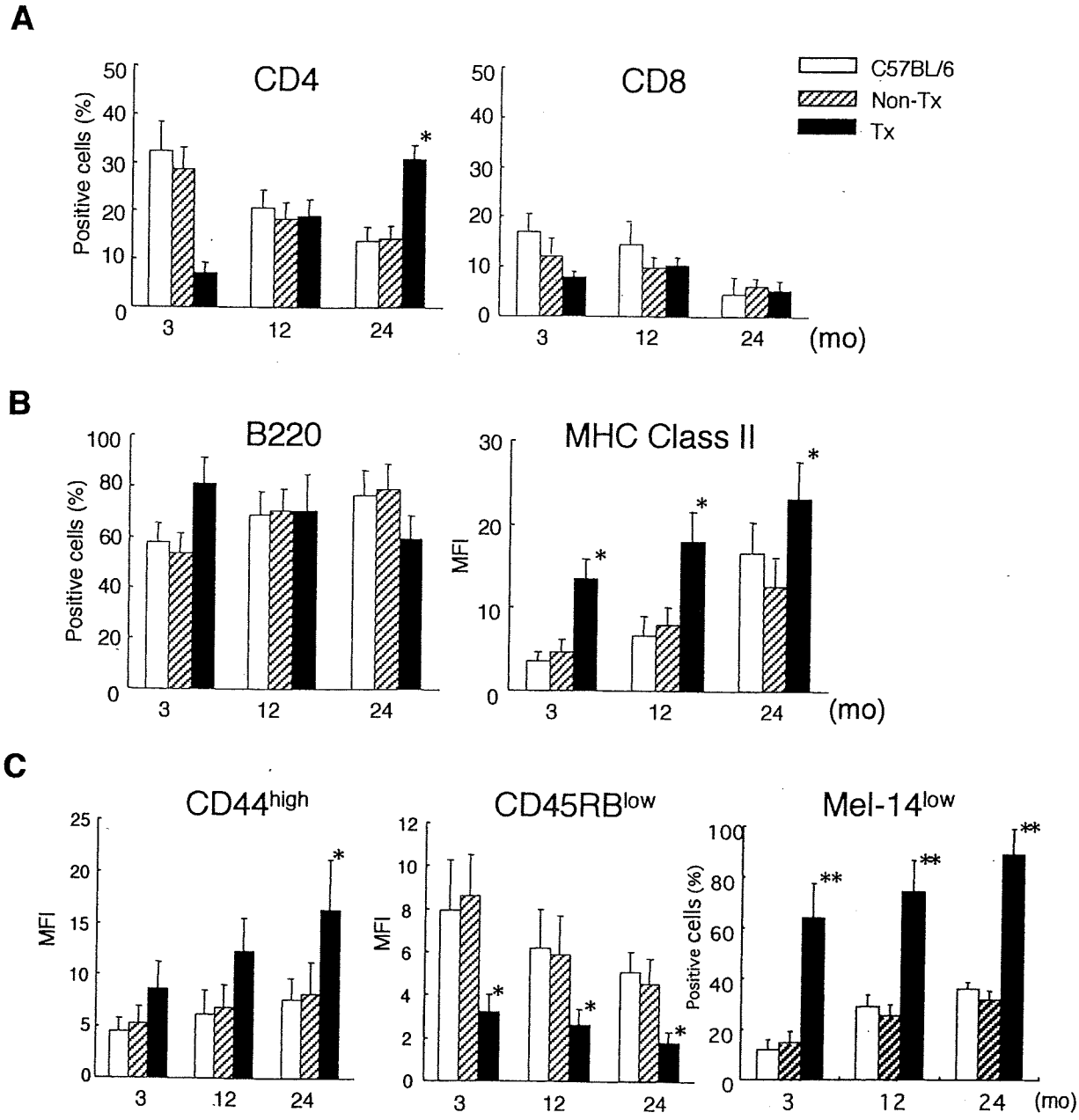

Figure 1. Age-related changes in activation markers. Shown are the results of the flow cytometric analysis of the CD4+,CD8+ T cell population, B220+ cells, class II major histocompatibility complex (MHC)–positive cells, and CD4+ T cells bearing activation markers in the spleens. Values are the mean and SD. **A**, An increase in the CD4+ T cell population, but not in the CD8+ T cell population, was detected in aged Sjögren's syndrome model mice (NFS/*sld* mice thymectomized on day 3 after birth, termed Tx mice). * = $P < 0.05$ versus nonthymectomized NFS/*sld* mice (non-Tx mice) or age-matched C57BL/6 control mice at age 24 months, by Student's *t*-test. **B**, Class II MHC–positive cells were significantly up-regulated in spleens with advancing age. * = $P < 0.05$ versus non-Tx or C57BL/6 control mice at all ages, by Student's *t*-test. No significant differences between groups were observed in the percentages of splenic B220+ cells. **C**, Significant up-regulation of CD4+ T cells bearing $CD44^{high}$, $CD45RB^{low}$, or Mel-14^{low} activation markers was observed in spleens from Tx mice with advancing age, but not in age-matched non-Tx or C57BL/6 control mice. * = $P < 0.05$; ** = $P < 0.01$, by Student's *t*-test. MFI = mean fluorescence intensity.

Serum samples were diluted (1:300) in 3% BSA in PBS, added to antigen-coated wells, incubated at 37°C for 1 hour, and washed 5 times with PBS containing 0.05% Tween 20. Subsequently, wells were incubated with peroxidase-conjugated goat anti-mouse Ig (BD PharMingen, San Diego, CA) for 1 hour and washed. We added 3,3′,5,5′-tetramethylbenzidine sub-

strate (Sigma, St. Louis, MO) and determined the absorbance spectrum with an automatic ELISA reader (Flow). Ig isotypes were assayed in the same manner using IgG1-specific and IgG2a-specific second-step conjugates and *p*-nitrophenyl phosphate substrate (Southern Biotechnology, Birmingham, AL). All assays were performed in duplicate and results were quantified against a standard curve obtained with the known positive control serum.

For the measurement of IgG-RF and IgM-RF, human IgG and IgM (Chemicon, Temecula, CA) were coated onto plates at 10 μg/ml in carbonate buffer, and the same procedures were followed as described above. Serum autoantibodies against α-fodrin fragments were detected using recombinant α-fodrin proteins. After coating with the recombinant α-fodrin protein in 96-well ELISA plates, biotinylated anti-mouse IgG (Vector, Burlingame, CA) was added as second antibody. Measurements of α-fodrin–specific autoantibodies were read with an automatic ELISA reader. For the measurement of serum antibodies to CII, native bovine CII was dissolved in 0.1*M* acetic acid at 1 mg/ml and diluted with 0.1*M* sodium bicarbonate at 10 μg/ml (pH 9.6). The microtiter plate was coated with 100 μl of CII antigen solution. After washing 3 times, 100 μl/well of serum samples that had been serially diluted in PBS/Tween 20/10% BSA and control serum were added and incubated for 1 hour at 37°C. After washing, peroxidase-conjugated goat anti-mouse IgG (at 1.4 μg/ml, 100 μl/well; Organon Teknika, Durham, NC) was added and incubated for 1 hour at 37°C. One hundred microliters of peroxidase-conjugated rabbit anti-mouse IgG (Zymed, San Francisco, CA) at a 1:1,000 dilution with PBS/Tween 20/10% BSA was added to detect anti-CII antibodies. A total of 100 μl *o*-phenylenediamine (0.5 mg/ml) dissolved in 0.1*M* citrate buffer (pH 5.0) containing 0.012% H_2O_2 was added, and the reaction was stopped using 8*N* H_2SO_4 (20 μl/well).

Proliferative T cell response. Single-cell suspensions of spleen cells were cultured in 96-well flat-bottomed microtiter plates (5×10^5/well) in RPMI 1640 containing 10% fetal calf serum, penicillin/streptomycin, and β-mercaptoethanol. Cells were cultured with 5 μg/ml of each recombinant α-fodrin protein (JS-1, 2.7A, and 3'DA), 5 μg/ml of bovine CII, and concanavalin A (EY Laboratories, San Mateo, CA) for 72 hours. During the last 8 hours of the 72-hour culture period, 1 μCi ^{3}H-thymidine was added per well, and the incorporated radioactivity was determined using an automated beta liquid scintillation counter (Aloka, Tokyo, Japan).

RESULTS

Analysis of the age-related changes in expression of activation markers. To clarify whether self-reactive T cells are spontaneously activated in aged SS model mice, we analyzed the CD4+,CD8+ T cell population, B220+ cells, class II major histocompatibility complex (MHC)–positive cells, and CD4+ T cells bearing activation markers in the spleens, by flow cytometry. The results showed that the CD4+ T cell population, CD4+ T cells bearing $CD44^{high}$, $Mel\text{-}14^{low}$, or $CD45RB^{low}$ activation markers, and class II MHC–positive cells were significantly up-regulated in the spleens from SS model mice with advancing age, but not in the spleens from age-matched non-Tx and B6 mice (Figures 1A–C). These data suggested that the spontaneously activating CD4+ T cells and class II–expressing antigen-presenting cells appear in the spleen with advancing age in the murine model of SS.

Age-related changes in joint histopathology. We examined the in vivo age-related changes in the development of extraglandular manifestations of autoimmune lesions in NFS/*sld* SS model (3d-Tx) mice compared with those in NFS/*sld* control (non-Tx) mice and age-matched B6 mice. Inflammatory lesions in aged SS model mice were observed in the joints and in several organs, including the lung, liver, and kidney, and the most prominent histopathologic abnormalities were observed in arthritic lesions. Destructive autoimmune arthritis developed in aging SS model mice, and these lesions became more aggravated with age from 6 months until 24 months. Histologic analysis of the knee joints was performed at ages 6, 12, 18, and 24 months for all of the experiments. Analysis of the histologic results indicated that the aged group had significantly greater subsynovial inflammation, synovial hyperplasia, pannus formation and cartilage erosion, bone destruction, and overall histologic abnormality (Figure 2A). Figure 2B shows photomicrographs of representative arthritic lesions from aging SS model mice at ages 18 and 24 months as well as the absence of such lesions in 24-month-old non-Tx and B6 mice. The effects observed in aged SS model mice included synovial hyperplasia, pannus formation, bone erosion, and infiltration of mononuclear cells into the subsynovial tissues. In contrast, mononuclear cell infiltration and bone and cartilage abnormalities were absent in age-matched control mice.

Age-related changes in cytokine profile and production of various autoantibodies. As measured by ELISA, culture supernatants from anti-CD3 mAb–stimulated splenic T cells obtained from SS model mice at ages 3, 12, and 24 months contained higher levels of IL-2 and IFNγ with advancing age, while levels of IL-4 and IL-10 were not observed to differ with advancing age (Figure 3A). We detected increased serum levels of RF (Figure 3B), anti-CII antibodies (Figure 3C), and anti-ssDNA antibodies (Figure 3D) in aging SS model mice but not in control mice. Moreover, we detected an increasing IgG2a:IgG1 ratio with advancing age in sera from SS model mice compared with sera from control mice (Figure 3E).

Immune responses against recombinant α-fodrin. To determine whether an immune response could be mounted against recombinant α-fodrin protein, the cDNA encoding human α-fodrin (JS-1, 1–1,784 bp;

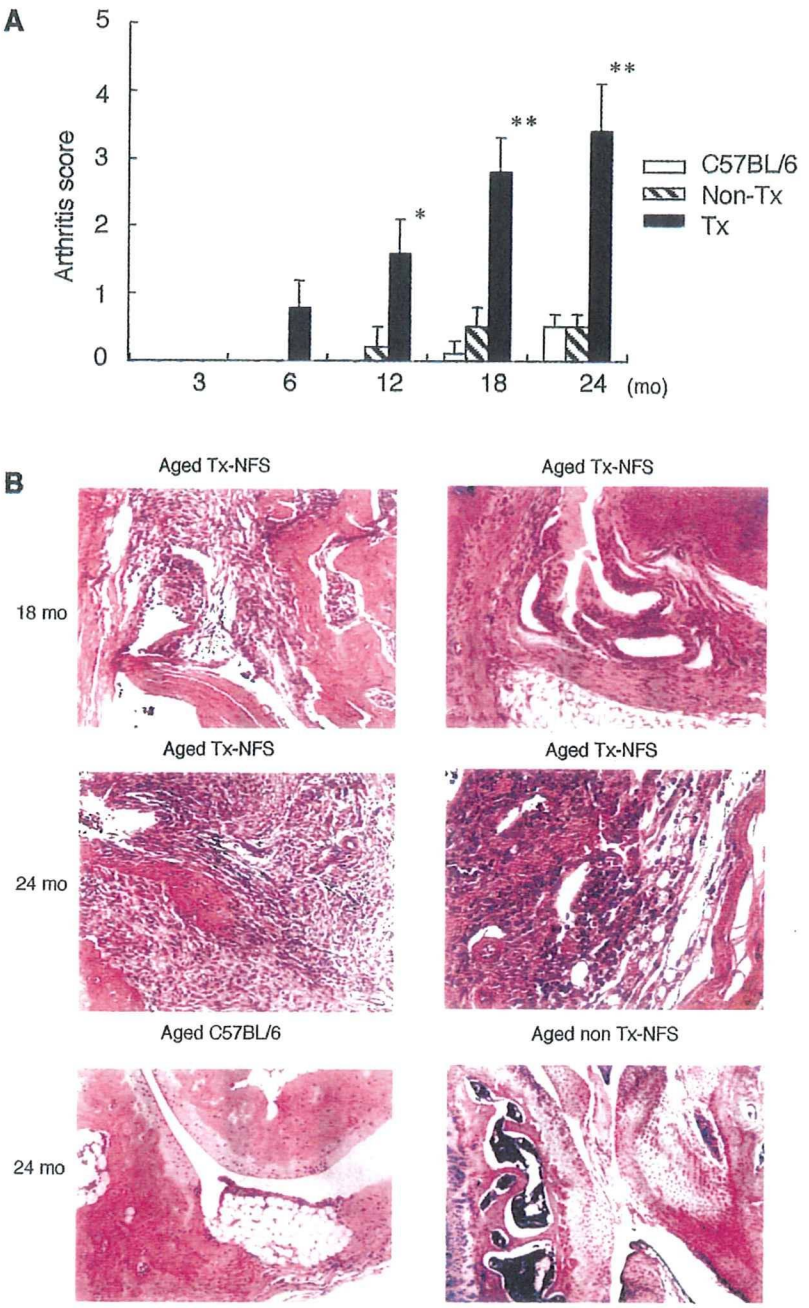

Figure 2. Age-related changes in joint histopathology. **A,** Effects of aging on joint histopathology in Sjögren's syndrome (SS) model mice. Shown are histologic scores of autoimmune arthropathy developed in aging SS model mice compared with those in age-matched non-Tx and C57BL/6 mice at ages 3, 6, 12, 18, and 24 months. Histologic evaluation of the knee joints was performed according to the methods of Edwards et al (see Materials and Methods) (27). Values are the mean and SD. $* = P < 0.05$; $** = P < 0.01$, by Student's *t*-test. **B,** Photomicrographs of representative arthritic lesions from aging SS model mice at ages 18 and 24 months. The histopathologic effects observed in these mice included pannus formation, synovial hyperplasia, and infiltration of mononuclear cells into the subsynovial tissues. In contrast, mononuclear cell infiltration and bone and cartilage abnormalities were absent in age-matched control mice at age 24 months. See Figure 1 for other definitions. (Hematoxylin and eosin stained; original magnification × 120.)

2.7A, 2,258–4,884 bp; 3′DA, 3,963–7,083 bp) was constructed by inserting cDNA into the *Eco* RI site of pGEX-4Ts (Figure 4A). A high titer of serum autoantibodies against the N-terminal α-fodrin fragment JS-1 (originally identified in primary SS model mice) was detected in both young and aged SS model mice

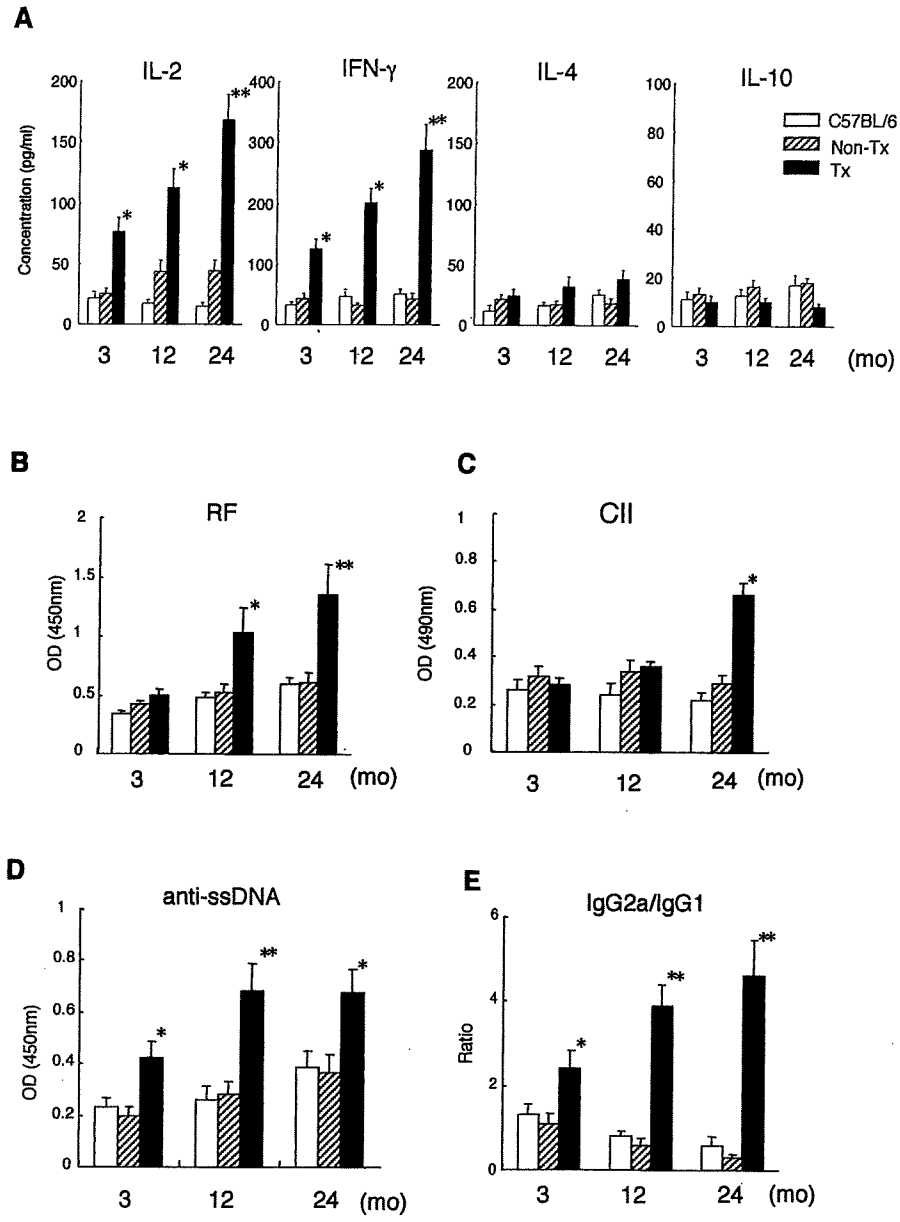

Figure 3. Age-related changes in cytokine profile and production of various autoantibodies. Values are the mean and SD. **A,** As measured by enzyme-linked immunosorbent assay, culture supernatants from anti-CD3 monoclonal antibody–stimulated splenic T cells obtained from aged Sjögren's syndrome (SS) model mice at ages 3, 12, and 24 months contained high levels of interleukin-2 (IL-2) and interferon-γ (IFNγ), while levels of IL-4 and IL-10 did not differ with advancing age. * = $P < 0.05$; ** = $P < 0.01$, by Student's *t*-test. **B,** Increased serum levels of rheumatoid factor (RF) were observed in aged SS model mice compared with those in control mice. * = $P < 0.05$; ** = $P < 0.01$, by Student's *t*-test. **C,** A significant increase in serum anti–type II collagen (anti-CII) antibodies was observed in aged SS model mice compared with control mice. * = $P < 0.05$ by Student's *t*-test. **D,** Significant increases in anti–single-stranded DNA (anti-ssDNA) antibodies were found at different ages in SS model mice compared with control mice. * = $P < 0.05$; ** = $P < 0.01$, by Student's *t*-test. **E,** An increasing IgG2a:IgG1 ratio with advancing age was detected in sera from SS model mice compared with control mice. * = $P < 0.05$; ** = $P < 0.01$, by Student's *t*-test. OD = optical density (see Figure 1 for other definitions).

by ELISA (Figure 4B). Moreover, autoantibody production against the C-terminus of the α-fodrin fragment (3′DA) was frequently detected in 12-month-old SS model mice (Figure 4B).

To address the role of autoantigen-reactive T cells, we examined the T cell proliferative responses against α-fodrin fragments (JS-1, 2.7A, and 3′DA) in the spleen cells at different ages. We detected significantly

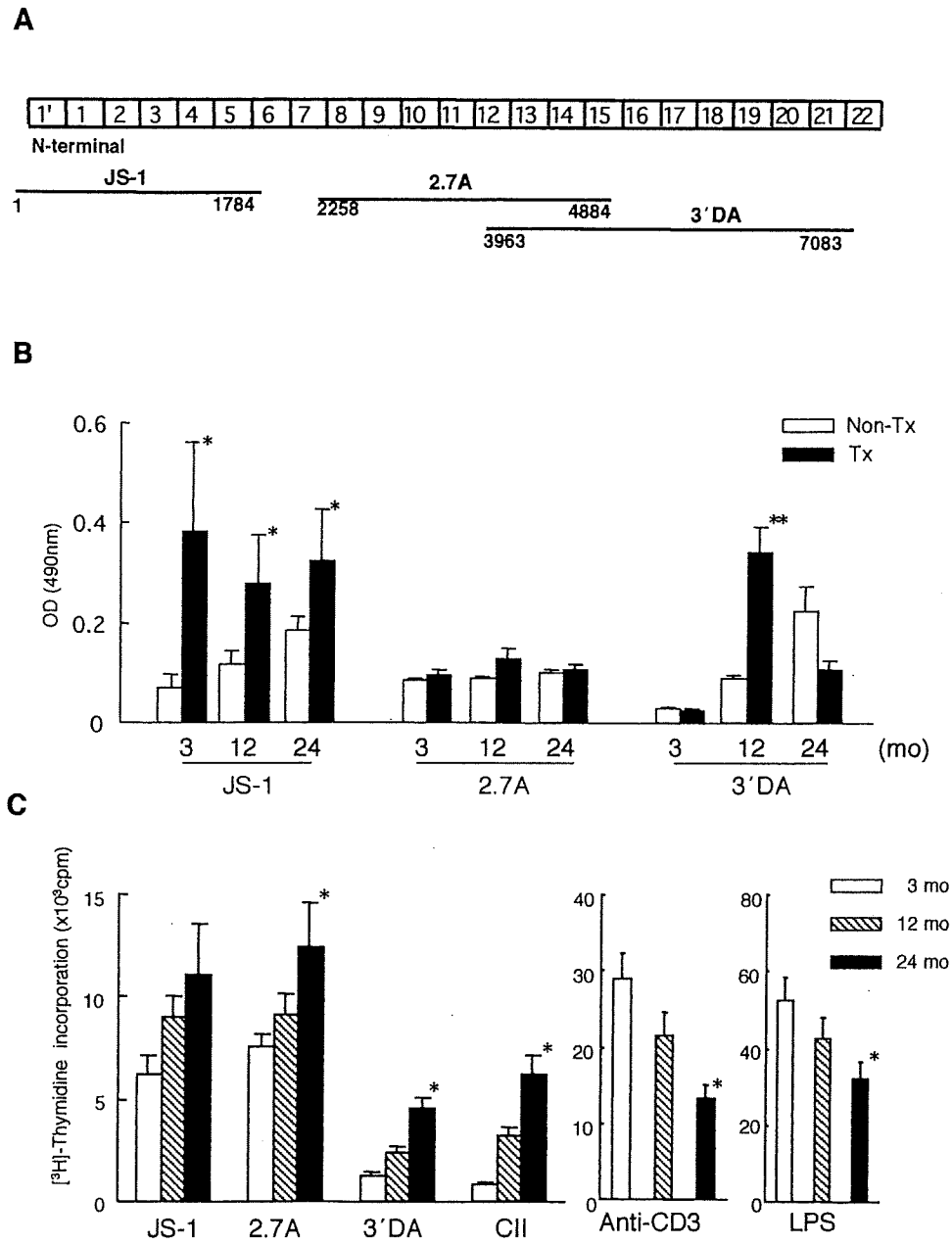

Figure 4. Immune responses against recombinant α-fodrin. **A**, Recombinant α-fodrin protein, the cDNA encoding human α-fodrin (JS-1, 1–1,784 bp; 2.7A, 2,258–4,884 bp; 3'DA, 3,963–7,083 bp), was constructed by inserting cDNA into the *Eco* RI site of pGEX-4Ts. **B**, A high titer of serum autoantibodies against the α-fodrin fragment JS-1, originally identified in primary SS model mice, was detected in both young and aged SS model mice by enzyme-linked immunosorbent assay. Moreover, autoantibody production against the C-terminus of the α-fodrin fragment (3'DA) was detected in 12-month-old SS model mice. Values are the mean and SD. * = $P < 0.05$; ** = $P < 0.01$, by Student's *t*-test. **C**, Significantly increased proliferation was detected in spleen cells from aged SS model mice stimulated with 2.7A and 3'DA protein. Moreover, a significant increase in CII-specific T cell proliferation was found in SS model mice with advancing age. In contrast, impaired proliferative responses were observed with advancing age upon stimulation with anti-CD3 and lipopolysaccharide (LPS). Values are the mean and SD of triplicate cultures. * = $P < 0.05$ by Student's *t*-test. See Figures 1 and 3 for other definitions.

increased proliferation in spleen cells from aged SS model mice stimulated with 2.7A and 3'DA protein (Figure 4C). We also examined the T cell proliferative responses against CII in the spleen cells at different ages. We found that the spleen cells in aged SS model mice showed a significant increase in CII-specific T cell

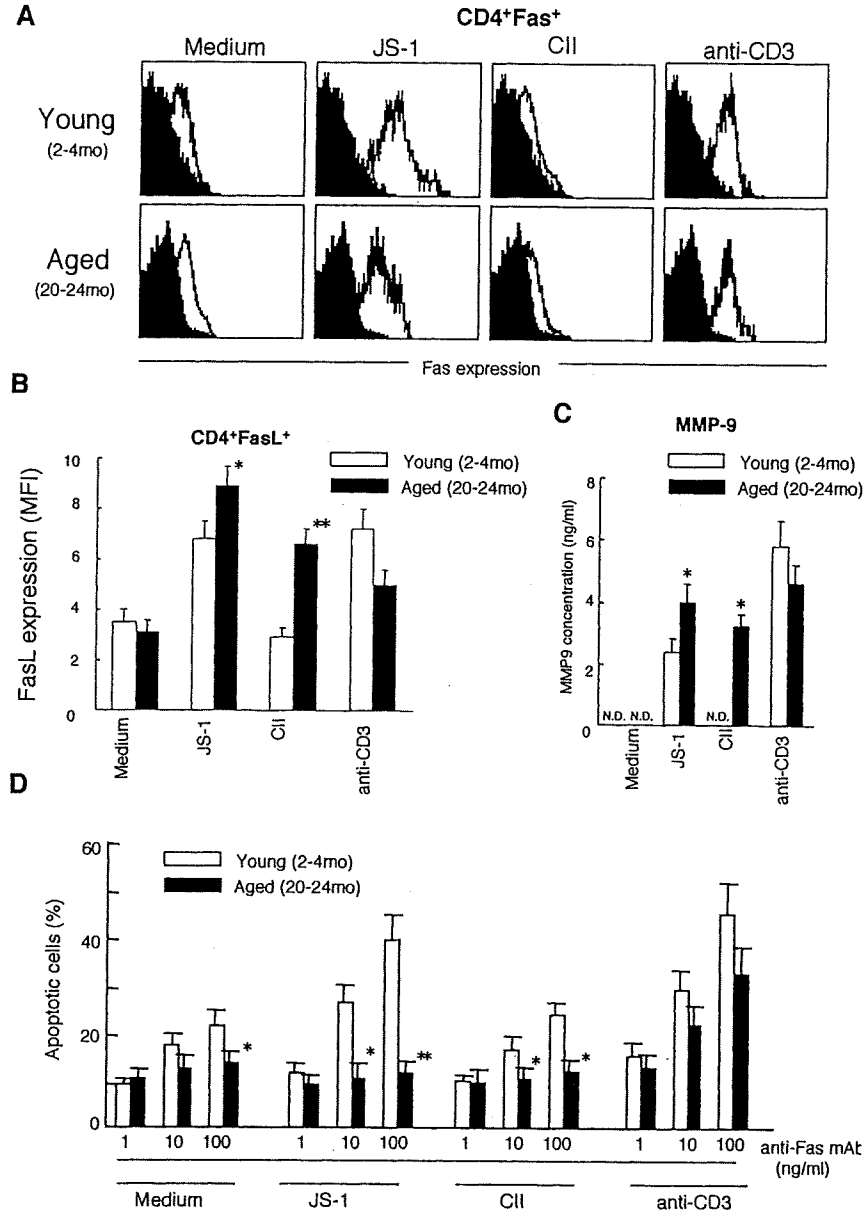

Figure 5. Expression of Fas, Fas ligand (FasL), and matrix metalloproteinase 9 (MMP-9). A, As shown by flow cytometry, an increased number of CD4+,Fas+ T cells was observed in JS-1–stimulated spleens from young SS model mice, but not from aged SS model mice. No significant difference was found in the numbers of CD4+,Fas+ T cells in CII-stimulated spleens from young versus aged SS model mice. B, A large proportion of CD4+ T cells expressing FasL was observed in spleens from aged SS model mice stimulated with either JS-1 or CII, but not in spleens stimulated with anti-CD3 monoclonal antibodies (mAb). Values are the mean and SD. * = $P < 0.05$; ** = $P < 0.01$, by Student's t-test. C, By enzyme-linked immunosorbent assay, an increased concentration of MMP-9 was detected in culture supernatant from JS-1– and CII-stimulated splenic T cells from aged SS model mice, but not in culture supernatant from anti-CD3 mAb–stimulated splenic T cells from young SS model mice. Values are the mean and SD. * = $P < 0.05$ by Student's t-test. D, Stimulation with autoantigens (JS-1 and CII) resulted in a significant, dose-dependent decrease in anti-Fas–induced CD4+ T cell apoptosis. Values are the mean and SD. * = $P < 0.05$; ** = $P < 0.01$, by Student's t-test. MFI = mean fluorescence intensity; ND = not detected (see Figure 3 for other definitions).

proliferation with advancing age (Figure 4C). In contrast, impaired proliferative responses were observed with advancing age upon stimulation with anti-CD3 and lipopolysaccharide. These data suggest that α-fodrin–reactive T cells may proliferate against a different antigenic epitope, which is followed by bystander T cell

activation, resulting in the development of autoimmune lesions in aged SS model mice.

Expression of Fas, FasL, and MMP-9. We next analyzed the numbers of Fas- and FasL-expressing splenic CD4+ T cells from young (ages 2–4 months) and aged (ages 20–24 months) SS model mice. An increased number of CD4+,Fas+ T cells was observed in spleens from young SS model mice, but not from aged SS model mice, stimulated with JS-1 (Figure 5A). No significant difference was found in the numbers of CD4+,Fas+ T cells in CII-stimulated spleens from young versus aged SS model mice (Figure 5A). A large proportion of CD4+ T cells expressing FasL was observed in spleens from aged SS model mice stimulated with either JS-1 or CII, but not in spleens stimulated with anti-CD3 mAb (Figure 5B). We previously detected a significantly increased concentration of MMP-9 in culture supernatant from JS-1–stimulated splenic T cells activated with anti-CD3 mAb from SS model mice (32). In the present study, we detected an increased concentration of MMP-9 in culture supernatant from JS-1– and CII-stimulated splenic T cells from aged SS model mice (Figure 5C). Moreover, it was demonstrated that autoantigen (JS-1 and CII) stimulation resulted in a significant, dose-dependent decrease in anti-Fas–induced CD4+ T cell apoptosis (Figure 5D), indicating the impairment of anti-Fas–induced T cell apoptosis in aged SS model mice. These data suggest that autoantigen stimulation may participate in immune dysregulation in the periphery in aged SS model mice.

DISCUSSION

We have used the NFS/*sld* mouse model of SS to study the age-related changes in the development of extraglandular manifestations of autoimmune lesions, and we have found that severe autoimmune arthritis developed with age in 12- and 24-month-old mice. An age-related dysregulation of immune functions in the murine model of SS resulted in a significant increase in serum levels of RF, anti-ssDNA antibodies, and anti-CII antibodies, and these changes increased with age.

Fas-mediated AICD is an important mechanism of peripheral T cell tolerance (7,33,34). Mice or humans lacking functional Fas or FasL display profound lymphoproliferative reactions associated with autoimmune disorders (35,36). We have previously demonstrated that Fas-mediated AICD is down-regulated by JS-1 autoantigen stimulation in spleen cells from SS model mice (32). In proteoglycan-induced arthritis, CD4+ T cells proliferate at a high rate in response to proteoglycan stimulation (37) and exhibit a Th1-type response (38). These observations suggest that a defect in AICD of autoreactive Th1 cells may contribute to the pathogenesis of the disease.

Our data demonstrated that splenic T cells from SS model mice contained higher levels of IL-2 and IFNγ with advancing age, and that a high titer of serum autoantibodies against α-fodrin autoantigen fragments (containing different epitopes that were originally identified in primary SS model mice) was frequently detected in young and aged SS model mice. We detected significantly increased proliferation in spleen cells from aged SS model mice stimulated with 2.7A and 3′DA protein. Our data suggest that α-fodrin autoantigen induces Th1 immune responses and accelerates disturbance of the Fas-mediated T cell apoptosis pathway in aged SS model mice.

We further observed that the spleen cells in aged SS model mice showed a significant increase in CII-specific T cell proliferation, which increased with age. CII, the main constituent of hyaline cartilage, has been proposed as one possible candidate autoantigen in rheumatoid arthritis (RA), because CII-specific antibodies are frequently found in RA patients and because an RA-like disease can be induced in certain mouse strains after immunization with CII. Our data showed a significant increase in production of serum autoantibodies against different fragments of α-fodrin autoantigen and against CII with aging, by ELISA. Moreover, significant proliferative responses against 2 α-fodrin fragments (2.7A and 3′DA) were observed in spleen cells from aged SS model mice, suggesting that bystander T cell activation may play an important role in the development of autoimmune lesions in these mice. It is possible that down-regulation of Fas-mediated AICD plays a major role in the accelerated development of autoimmune lesions with aging in the murine model of SS.

Epitope spreading has been generally proposed to contribute to the chronic pathogenesis of T cell–mediated autoimmune diseases, including experimental autoimmune encephalomyelitis (EAE) (39,40) and spontaneous diabetes in the nonobese diabetic mouse (41,42). However, it remains unclear whether T cells specific for endogenous epitopes play a significant pathologic role in tissue damage during the clinical episodes. CD4+ T cells are susceptible to AICD induced through T cell receptor (TCR)–mediated recognition of allogeneic class II MHC molecules (43,44). Our data demonstrate that autoantigen (JS-1 and CII) stimulation results in a significant, dose-dependent decrease in anti-Fas–induced CD4+ T cell apoptosis. In addition,